The Magnetic Memory of Titan's Ionized Atmosphere

C. Bertucci, *et al.*

Science **321**, 1475 (2008);
DOI: 10.1126/science.1159780

Science (print ISSN 0036-8075; online ISSN 1095-9203) is published weekly, except the last week in December, by the American Association for the Advancement of Science, 1200 New York Avenue NW, Washington, DC 20005.

the observed time and length scales (~100 ns judging from the micrometer-scale sharpness of the reaction front in Fig. 2A and the 13-m/s propagation speed). These time and length scales are not consistent with an alternative hypothesis that the structures arise from purely solid-state diffusive processes, which are orders of magnitude too slow, even at 1700 K (*26*).

The dark intensity between the cells fades away in the last micrograph of the series in Fig. 2, at a point in time where the reaction is long since complete. The solid solubility range of the NiAl B2 phase increases as the temperature drops (*22*), so that at room temperature nearly all of the excess Ni could be reabsorbed into a stable homogeneous B2 structure with a Ni:Al ratio close to 3:2. Post-mortem TEM examination indicates that this happens in nearly all cases, with frozen-in structures (such as those in fig. S5) being rare exceptions associated with defects. The cellular morphology is not normally present at completion.

We have obtained single-pulse nanosecond-scale TEM data in both diffraction and imaging modes, which are necessary to study the propagation and behavior of energetic nanolaminates in situ. With the use of 15-ns imaging, we have observed transient structures produced by the self-propagating high-temperature synthesis, revealing lines of mass-thickness contrast due to cellular phase formation of an ordered B2 NiAl phase and liquid. At such high formation temperatures (~1700 K), these materials are now known to exhibit transverse self-ordering reminiscent of cellular binary solidification mechanisms. We have established that the DTEM is proficient for nanosecond science in a TEM for direct nanoscale characterization of irreversible, dynamic phenomena. It is notable and exciting to find spontaneous, rapid formation of ordered structures in materials far from equilibrium, which is also an important step for essential comprehension of RMLF performance in applications.

References and Notes

1. P. E. Batson, N. Dellby, O. L. Krivanek, *Nature* **418**, 617 (2002).
2. O. L. Krivanek, N. Dellby, A. R. Lupini, *Ultramicroscopy* **78**, 1 (1999).
3. M. Haider *et al.*, *Ultramicroscopy* **75**, 53 (1998).
4. A. M. Minor, E. T. Lilleodden, E. A. Stach, J. W. Morris, *J. Electron. Mater.* **31**, 958 (2002).
5. R. Sharma, Z. Iqbal, *Appl. Phys. Lett.* **84**, 990 (2004).
6. E. D. Boyes, P. L. Gai, *Ultramicroscopy* **67**, 219 (1997).
7. M. R. Armstrong, B. W. Reed, B. R. Torralva, N. D. Browning, *Appl. Phys. Lett.* **90**, 114101 (2007).
8. P. B. Hirsch, R. W. Horne, M. J. Whelan, *Philos. Mag.* **1**, 677 (1956).
9. S. Iijima, *Nature* **354**, 56 (1991).
10. W. E. King *et al.*, *J. Appl. Phys.* **97**, 111101 (2005).
11. T. LaGrange *et al.*, *Appl. Phys. Lett.* **89**, 044105 (2006).
12. O. Bostanjoglo, R. Elschner, Z. Mao, T. Nink, M. Weingartner, *Ultramicroscopy* **81**, 141 (2000).
13. T. LaGrange, G. H. Campbell, P. E. A. Turchi, W. E. King, *Acta Mater.* **55**, 5211 (2007).
14. U. Anselmitamburini, Z. A. Munir, *J. Appl. Phys.* **66**, 5039 (1989).
15. A. J. Gavens, D. Van Heerden, A. B. Mann, M. E. Reiss, T. P. Weihs, *J. Appl. Phys.* **87**, 1255 (2000).
16. J. C. Trenkle, J. Wang, T. P. Weihs, T. C. Hufnagel, *Appl. Phys. Lett.* **87**, 153108 (2005).
17. J. Wang *et al.*, *J. Appl. Phys.* **95**, 248 (2004).
18. S. J. Zhao, T. C. Germann, A. Strachan, *J. Chem. Phys.* **125**, 164707 (2006).
19. T. P. Weihs, in *Handbook of Thin Film Process Technology*, D. A. Glocker, S. I. Shan, Eds. (Institute of Physics Publishing, Bristol, UK, 1998), p. F7.1.
20. J. S. Langer, *Rev. Mod. Phys.* **52**, 1 (1980).
21. B. E. Sundquist, *Acta Metall.* **16**, 1413 (1968).
22. M. F. Singleton, J. L. Murray, P. Nash, in vol. 1 of *Binary Alloy Phase Diagrams*, T. B. Massalski, Ed. (ASM International, Metals Park, OH, 1990), pp. 181–184.
23. C. Michaelsen, K. Barmak, T. P. Weihs, *J. Phys. D Appl. Phys.* **30**, 3167 (1997).
24. L. Perring, J. J. Kuntz, F. Bussy, J. C. Gachon, *Intermetallics* **7**, 1235 (1999).
25. Lattice-expansion measurement was determined by Reitveld analysis of the diffraction data.
26. H. Wei, X. Sun, Q. Zheng, H. Guan, Z. Hu, *Acta Mater.* **52**, 2645 (2004).

27. This work was performed under the auspices of the U.S. Department of Energy (DOE) by LLNL and supported by the Office of Science, Office of Basic Energy Sciences, Division of Materials Sciences and Engineering of the DOE under contract DE-AC52-07NA27344. J.S.K. is supported by the Lawrence Scholar Program at LLNL. The authors thank K. J. M. Blobaum and T. W. Barbee for valuable discussions, P. Ramsey for materials fabrication, and R. M. Shuttlesworth and B. J. Pyke for their support and expertise in mechanical and laser technologies.

Supporting Online Material

www.sciencemag.org/cgi/content/full/321/5895/1472/DC1
Figs. S1 to S5
Movie S1

9 June 2008; accepted 23 July 2008
10.1126/science.1161517

The Magnetic Memory of Titan's Ionized Atmosphere

C. Bertucci,[1]*† N. Achilleos,[2,3] M. K. Dougherty,[1] R. Modolo,[4] A. J. Coates,[5,3] K. Szego,[6] A. Masters,[1] Y. Ma,[7] F. M. Neubauer,[8] P. Garnier,[9] J.-E. Wahlund,[9] D. T. Young[10]

After 3 years and 31 close flybys of Titan by the Cassini Orbiter, Titan was finally observed in the shocked solar wind, outside of Saturn's magnetosphere. These observations revealed that Titan's flow-induced magnetosphere was populated by "fossil" fields originating from Saturn, to which the satellite was exposed before its excursion through the magnetopause. In addition, strong magnetic shear observed at the edge of Titan's induced magnetosphere suggests that reconnection may have been involved in the replacement of the fossil fields by the interplanetary magnetic field.

The absence of a substantial intrinsic magnetic field at Titan results in a direct interaction between the moon's chemically complex atmosphere and its plasma environment (*1*). This interaction consists of electromagnetic coupling between charged particles resulting from the ionization of Titan's atmosphere and neutral corona, and the external wind of magnetized plasma. As external plasma approaches Titan, it is mass-loaded by these locally produced ions (*2*) and its speed progressively decreases. Because the plasma is virtually collisionless, a magnetic field is frozen into the plasma, causing external field lines to drape around the moon. Magnetic field lines then pile up near the sub-flow point and stretch along the flow direction in the flanks and the downstream sector, creating an induced magnetosphere and magnetotail. In a Titan-centered frame of reference, the magnetotail consists of "away" and "toward" lobes containing, respectively, draped field lines parallel and antiparallel to the external flow (*3*, *4*). This interaction leads to the removal of ionized atmospheric constituents as they acquire the linear momentum lost by the external flow (*5*).

Titan orbits Saturn at an average distance of 20.2 Saturn radii [1 Saturn radius (R_S) = 60,268 km], spending most of its time in Saturn's partially corotating magnetospheric flow (Fig. 1A). This flow, consisting of charged particles from sources such as the E ring and Enceladus (*6*), transports Saturn's magnetic field, which encounters Titan at speeds of ~100 km/s (*1*). Hence, the angle between the magnetospheric flow and the solar photons responsible for the ionization of Titan's atmosphere—and therefore the interaction—depends on the moon's local time with respect to Saturn [Saturn local time (SLT)] (*7*). At SLT near noon, Titan can also interact with the shocked solar wind and the interplanetary magnetic field (IMF) during periods of high solar wind dynamic pressure (P_{SW}) (*8*), as the pressure balance at the magnetopause occurs at lower kronocentric distances, leaving Titan in the magnetosheath (Fig. 1B).

[1]Space and Atmospheric Physics Group, Imperial College London, The Blackett Laboratory, Prince Consort Road, London SW7 2AZ, UK. [2]Atmospheric Physics Laboratory, Department of Physics and Astronomy, University College London, Gower Street, London WC1E 6BT, UK. [3]Centre for Planetary Sciences, University College London, UK. [4]Department of Physics and Astronomy, University of Iowa, 613 Van Allen Hall, Iowa City, IA 52242–1479, USA. [5]Mullard Space Science Laboratory, University College London, Holmbury St. Mary, Dorking, Surrey RH5 6NT, UK. [6]KFKI Research Institute for Particle and Nuclear Physics, Konkoly Thege Street 29-33, Building III, H-1121 Budapest, Hungary. [7]Institute of Geophysics and Planetary Physics, University of California Los Angeles, Los Angeles, CA 90025, USA. [8]Institute for Geophysics and Meterology, Köln University, 50923 Köln, Germany. [9]Swedish Institute of Space Physics, Box 537, SE-751 21 Uppsala, Sweden. [10]Southwest Research Institute, Post Office Box 28510, San Antonio, TX 78227–1301, USA.

*Present address: Instituto de Astronomica y Fisica del Espacio, Ciudad Universitaria, Buenos Aires, Argentina.
†To whom correspondence should be addressed. E-mail: cbertucci@iafe.uba.ar

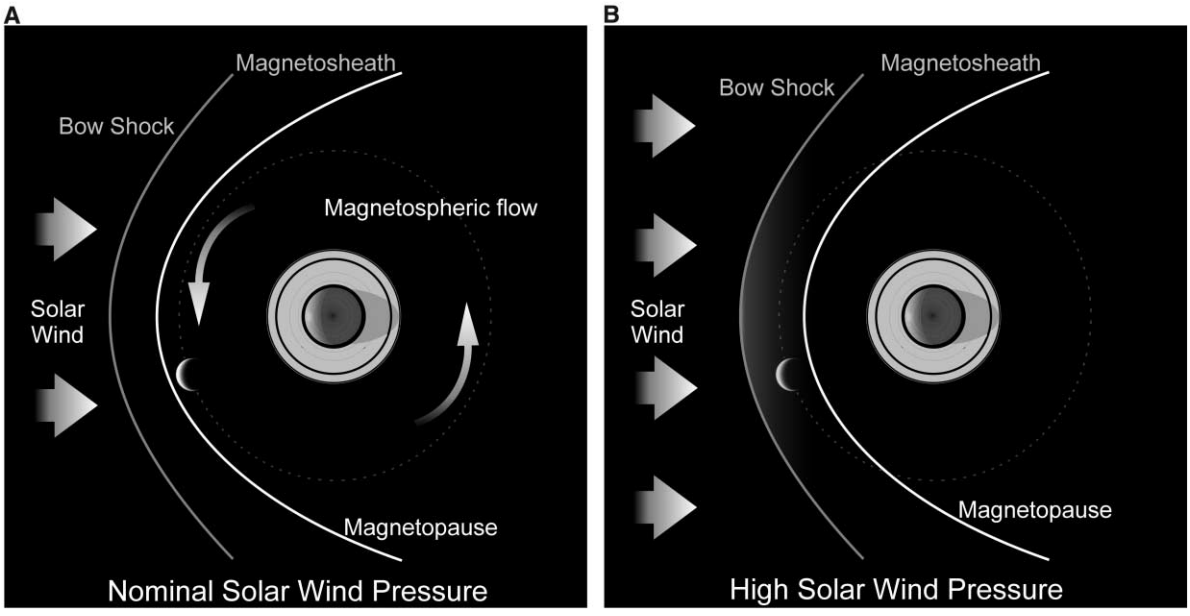

Fig. 1. Sketch describing how Titan's plasma interaction depends on solar wind pressure. Under nominal solar wind conditions, Titan interacts with Saturn's rotating magnetosphere (**A**). When solar wind pressure is high, Titan exits into Saturn's magnetosheath (**B**). Both panels indicate Titan's position during T32.

Fig. 2. (**Top**) Cassini magnetic field data on 13 June 2007 in spherical KSMAG coordinates. The encounters with the oscillating kronian magnetopause and bow shock are indicated with the letters A to C and D to F, respectively. |*B*| is the magnetic field strength. Cassini's kronocentric distance is indicated beneath the plots. (**Bottom**) Magnetic field data in spherical TIIS coordinates (from MAG), plasma density (N_e) (from RPWS/LP), and electron count rate per energy channel (from CAPS/ELS) during the T32 flyby. Magnetopause crossing C, CA, and the entry (I) and exit (II) of the fossil field region are indicated. Cassini's altitude above Titan is indicated beneath the plots.

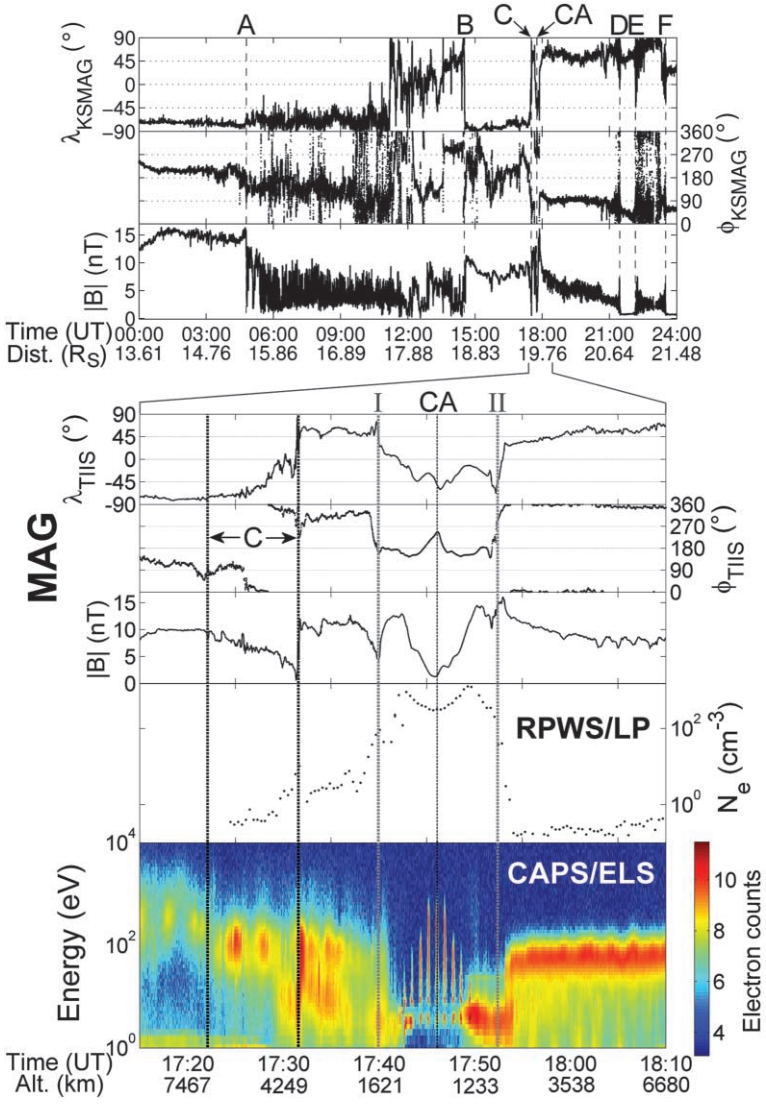

During every in situ observation made from Voyager 1 (*3*) through Cassini close flyby 31 (T31), Titan was inside the kronian magnetosphere. However, during T32 on 13 June (day 164) 2007, Cassini encountered Titan while it was in the shocked solar wind. Observations of the plasma environment showed layers of remnant kronian magnetic fields to which Titan had been exposed a few minutes before, revealing how this field interacts with the IMF.

T32 took place at 13.6 hours SLT, close to the Saturn-Sun line, when the spacecraft was outbound from the kronian system. In the Titan-centered frame, Cassini's trajectory was almost parallel to the Saturn-Sun direction and north of the moon's orbital plane. Closest approach (CA) occurred at 17:46:32 universal time (UT) (*9*) at an altitude of 975 km over the north pole. As a result, Cassini first explored the near-Saturn side of Titan's induced magnetosphere, then flew through the collisional ionosphere and emerged on the side facing away from the planet.

The T32 encounter occurred after a series of compressions and expansions of Saturn's magnetopause (at speeds much higher than Cassini's) in response to strong variations in P_{SW}. These oscillations are noticeable in the Cassini magnetometer (MAG) (*10*) data in the spherical KSMAG coordinate system (*11*) aligned with Saturn's magnetic dipole (Fig. 2, top panel). Early on day 164, Cassini was immersed in a typical north/south kronian magnetic field. Then the magnetosphere contracted because of an increase in P_{SW}. The receding magnetopause passed Cassini around 04:47 (point A) at a distance of ~15.4 R_S from Saturn. A model of the magnetopause based on pressure balance (*12*, *13*) suggests that P_{SW} was ~0.08 nPa (more than five times the average value). From that moment, Titan was also outside the magnetosphere. Furthermore, if the same dependence on P_{SW} is applied to the bow shock (*14*), Titan was in the supersonic solar wind at the time of A. After A, Cassini spent almost 10 hours outside Saturn's magnetosphere. Meanwhile, the magnetopause stopped contracting and expanded once again, reaching Cassini around 14:32 (point B). Cassini was then within the magnetosphere for ~3 hours until it encountered, one last time, a retreating magnetopause around 17:25 (point C), more than 20 min before CA. The magnetic field disturbance generated by Titan was observed by Cassini ~10 min after C. After ~11:00, the IMF was mainly northward, leading to strong magnetic shear at crossings B and C.

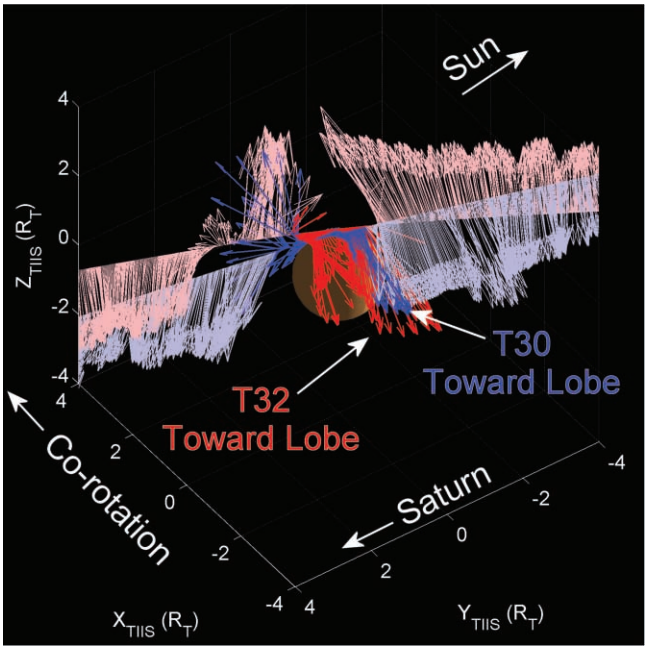

Fig. 3. Magnetic field measurements along the trajectories of flybys T30 (blue) and T32 (red) in TIIS coordinates. The draped magnetic fields of Titan's induced magnetosphere are highlighted in bright colors. Light-colored blue and red arrows indicate the unperturbed ambient field.

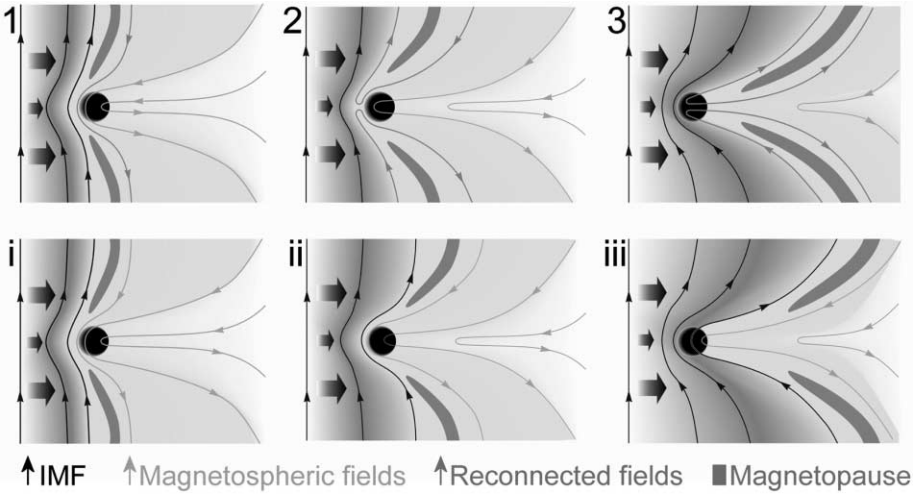

Fig. 4. Simplified schematics showing, from the same initial scenario and in three stages, possible reconfigurations of the magnetic field near Titan during T32. (**Top**) Saturn's magnetopause opens as a result of reconnection between the kronian fossil fields and the IMF (1), and reconnected field lines are carried downstream (2 and 3). (**Bottom**) The absence of reconnection (i) results in a closed magnetopause that sweeps across Titan's induced magnetosphere (ii and iii). The shocked solar wind travels from left to right. The formation of the fossil fields and possible tail reconnection are not shown because of the geometrical complexity of the process.

The combined capabilities of Cassini MAG, the Radio and Plasma Wave Science instrument (RPWS) (*15*), and the Cassini Plasma Spectrometer/Electron Spectrometer (CAPS/ELS) (*16*) provide a detailed description of the plasma near Titan (Fig. 2, bottom panel). Magnetic field data are shown in the spherical Titan interaction (TIIS) coordinate system defined from the nominal kronian corotation flow (*4*, *17*). In Cassini's frame of reference, the magnetopause crossing C displayed a thick boundary layer, where the magnetospheric and the magnetosheath plasmas coexisted, whereas the magnetic field rotated northward by 156°. These signatures are typical of local magnetopause reconnection events previously observed at Saturn (*18*). Also within C, ELS and the RPWS Langmuir probe (LP) detected (from 17:30) a less energetic (10-eV) electron population that probably originated from Titan. After C (between 17:32 and 17:38, and after 17:53), the magnetic field was predominantly northward, confirming that Titan was in the IMF. The mixed magnetosphere/magnetosheath plasma signature continued until 17:38.

Around 17:41 and 17:53 (altitudes of 1400 and 1740 km, respectively), the sudden drop in 100- to 1000-eV electron count rates indicates that the external flow was strongly decelerated and deflected near Titan, as its cold plasma began to dominate. Simultaneously, the plasma density increased above 100 cm^{-3} and the frequency of collisions became comparable to the ion gyrofrequency. As a result, only electrons remained magnetized and deposited the magnetic field in the induced magnetosphere via convective pileup. These electrons had lost most of their momentum, making the magnetic flux tube convection time extremely long as compared to that at higher altitudes.

From 17:43:30 to 17:49:00 (below an altitude of 1100 km), extremely weak fields indicate that Cassini entered Titan's collisional ionosphere, where magnetic diffusion dominated over convec-

tion. A minimum value of 1.25 nT was measured a few seconds before CA and below the ionospheric peak around 17:42 and 17:50 (altitudes of 1270 and 1200 km, respectively).

Between approximately 1200 and 1600 km altitude (points I and II), the draped magnetic field was antiparallel to the corotation direction (the toward lobe). Because Cassini was at northern latitudes, this lobe corresponds to the draping of a field that was initially southward. However, the IMF surrounding Titan was clearly northward, and there is no possibility that such an orientation could lead to a toward lobe at northern latitudes. A comparison between the average field in Titan's magnetotail during T32 with that in the toward lobe during three north latitude flybys with almost identical geometries (T28, T29, and T30) inside Saturn's magnetosphere shows that these directions differed by as little as 28°. The fields in the toward lobes of flybys T32 and T30 (Fig. 3) display high similarity (8° between averages).

In the absence of an internal field, the fields just above Titan's collisional ionosphere are draped kronian magnetospheric fields deposited within Titan's induced magnetosphere before the moon's magnetosheath excursion. These fields are effectively frozen or "fossilized" in the near-Titan noncollisional plasma as a result of mass loading by cold ions [notably N_2^+ (*19*)] from Titan's exosphere below 1600 km, dramatically reducing the transit speed of magnetic flux tubes. As Titan entered the magnetosheath, it encountered shocked solar wind traveling along the Sun-Saturn direction. This flow transported IMF field lines, which piled up and draped around the layers of fossilized fields, as shown by the monotonic change in the magnetic field strength after 17:53. Thus, draped field lines at higher altitudes moved at higher speeds, reflecting more recently sampled magnetic environments.

The detection of kronian fossil fields during T32 occurred because their convection time was longer than the time that Titan was exposed to the IMF. In the early hours of day 164, Titan was immersed in the magnetosheath longer than Cassini (9 hours, 45 min), because the spacecraft was inside Titan's orbit. For the same reason, Titan was within Saturn's magnetosphere for a shorter time than the interval from B to C. However, this was long enough to replenish Titan's induced magnetosphere with kronian fields after the first magnetosheath excursion. Hence, if Titan was within Saturn's magnetosphere for some time between B and C, and if the replenishment time was the same for the IMF and magnetospheric fields, the time spent by Titan in Saturn's magnetosphere between B and C should have been longer than that between C and CA. As a result, the lifetime of the kronian fossil fields was between ~20 min and ~3 hours. These conclusions support previous theoretical estimations within Saturn's magnetosphere (*20*).

The fossil fields could have been removed via diffusion into the collisional ionosphere, convection around the ionosphere into the magnetotail, and reconnection with the IMF. The magnetic shear at locations I and II (111° and 162°, respectively) and the magnetic field variance suggest that reconnection could have occurred during T32. In this scenario (Fig. 4, top panels), Titan could have opened Saturn's magnetopause, and the field reconfiguration could have been similar to that proposed for disconnection events at comets (*21*). Initial real-time modeling supports this interpretation.

However, previous simulations (*20*) indicate that at these altitudes, the plasma density was too low for electrons to be demagnetized. In such a case (Fig. 4, bottom panels), reconnection would not have occurred, and the fossilized fields could have been either diffused into the collisional ionosphere or transported downstream by ambipolar electric fields (*22*) without affecting the magnetic structure of Saturn's magnetopause.

The bow-shock crossings D, E, and F at kronocentric distances of 20.8, 21.0, and 21.4 R_S (Fig. 2, top panel) suggest magnetopause standoff distances around 16 R_S. Hence, it is likely that after T32, Titan remained within Saturn's magnetosheath at least until 23:30, when the fossil fields should have been entirely removed.

References and Notes

1. F. M. Neubauer, D. A. Gurnett, J. D. Scudder, R. E. Hartle, in *Saturn*, T. Gehrels, M. S. Matthews, Eds. (Univ. of Arizona Press, Tucson, AZ, 1984), pp. 760–787.
2. J.-E. Wahlund *et al.*, *Science* **308**, 986 (2005).
3. N. F. Ness, M. H. Acuña, K. W. Behannon, *J. Geophys. Res.* **87**, 1369 (1982).
4. H. Backes *et al.*, *Science* **308**, 992 (2005).
5. K. Szego *et al.*, *Geophys. Res. Lett.* **34**, L24S03 (2007).
6. M. G. Kivelson, *Science* **311**, 1391 (2006).
7. SLT is measured from the noon meridian in the direction of Saturn's rotation.
8. $P_{SW} = \rho v^2$, where ρ and v are the solar wind density and speed, respectively.
9. All times are expressed in UT.
10. M. K. Dougherty *et al.*, *Space Sci. Rev.* **114**, 331 (2004).
11. In the Saturn-centered spherical solar magnetic coordinate system (KSMAG), the polar axis coincides with planet's magnetic axis and λ_{KSMAG} and ϕ_{KSMAG} are, respectively, the magnetic field latitude and azimuth ($\phi_{KSMAG} = 0$ corresponds to the magnetic noon meridian).
12. $R_{MP} = P_{SW}^{-1/4.3}$, where R_{MP} is the magnetopause's standoff distance.
13. C. S. Arridge *et al.*, *J. Geophys. Res.* **111**, A11227 (2006).
14. A. Masters *et al.*, *J. Geophys. Res.* 10.1029/2008JA013276 (2008).
15. D. A. Gurnett *et al.*, *Space Sci. Rev.* **114**, 395 (2004).
16. D. T. Young *et al.*, *Space Sci. Rev.* **114**, 1 (2004).
17. In the Titan-centered spherical ionospheric interaction coordinate system (TIIS), the equatorial plane contains the direction to Saturn (Y_{TIIS}) and that of the nominal corotation flow (X_{TIIS}). λ_{TIIS} and ϕ_{TIIS} are, respectively, the latitude and azimuth (measured from X_{TIIS} toward Y_{TIIS}).
18. H. J. McAndrews *et al.*, *J. Geophys. Res.* **113**, A04210 (2008).
19. R. E. Hartle *et al.*, *Geophys. Res. Lett.* **33**, L08201 (2006).
20. H. Backes, thesis, University of Cologne, Germany (2005).
21. M. B. Niedner, J. C. Brandt, *Astrophys. J.* **223**, 655 (1978).
22. A. J. Coates *et al.*, *Geophys. Res. Lett.* **34**, L24S05 (2007).

23. We thank A. Balogh, T. Horbury, W. S. Kurth, C. Mazelle, S. J. Schwartz, and C. T. Russell for useful discussions, and N. Powell for artwork. C.B. was supported by a Science and Technology Facilities Council Postdoctoral Fellowship.

29 April 2008; accepted 28 July 2008
10.1126/science.1159780

Postseismic Relaxation Along the San Andreas Fault at Parkfield from Continuous Seismological Observations

F. Brenguier,[1,2]* M. Campillo,[2] C. Hadziioannou,[2] N. M. Shapiro,[1] R. M. Nadeau,[3] E. Larose[2]

Seismic velocity changes and nonvolcanic tremor activity in the Parkfield area in California reveal that large earthquakes induce long-term perturbations of crustal properties in the San Andreas fault zone. The 2003 San Simeon and 2004 Parkfield earthquakes both reduced seismic velocities that were measured from correlations of the ambient seismic noise and induced an increased nonvolcanic tremor activity along the San Andreas fault. After the Parkfield earthquake, velocity reduction and nonvolcanic tremor activity remained elevated for more than 3 years and decayed over time, similarly to afterslip derived from GPS (Global Positioning System) measurements. These observations suggest that the seismic velocity changes are related to co-seismic damage in the shallow layers and to deep co-seismic stress change and postseismic stress relaxation within the San Andreas fault zone.

Information about the stress variations in deeper parts of continental faults can be obtained by studying source properties of microearthquakes (*1*). Changes in seismic velocities measured by using repeated natural and active seismic sources can also provide information about rock damage and healing at depth after large earthquakes (*2*, *3*) or about stress changes in seismogenic zones (*4*). The main limitation of these types of measurements, however, is the episodic nature of their seismic sources, which prevents continuous monitoring of crustal properties.

We used continuous measurements of ambient seismic noise to recover continuous variations of seismic velocities within the crust along the San Andreas fault (SAF) near Parkfield, California. With this approach, the cross-correlation function of ambient seismic noise computed between a pair of receivers converges toward the response of Earth between the receivers (the so-called Green's function). Essentially this function represents the seismogram that would be recorded at one of the receivers if a source were acting at the second (*5*, *6*). The